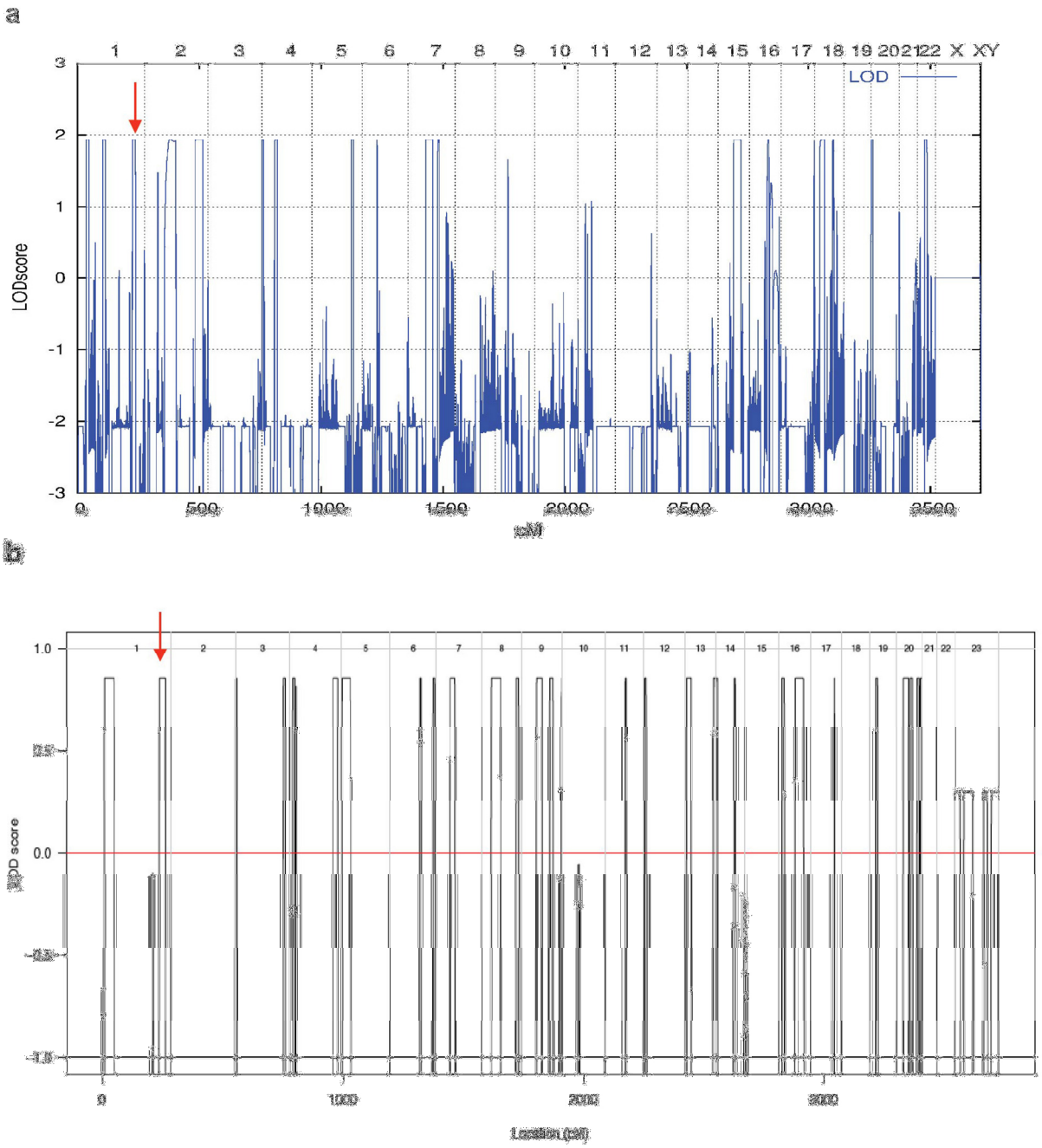

Supplementary Figure 1

Parametric genome-wide linkage analysis.

(**a**) LOD scores obtained from parametric linkage analysis of family A. Linkage was calculated using 20,044 selected SNP markers from the Affymetrix SNP Array 6.0. LOD scores calculated with ALLEGRO are given along the y-axis relative to genomic position in cM (centiMorgan) on the x-axis. Chromosomes are concatenated from p-ter to q-ter from left to right. Red arrow indicates position of *SPRTN*. (b) LOD scores

obtained from parametric linkage analysis of Family B under a recessive genetic model. LOD scores are on the y-axis and cumulative genomic position in cM (centiMorgan) on x-axis. The vertical lines depict the boundaries of each chromosome. The maximum theoretical autosomal LOD score of 0.85 is achieved at 29 sites, while the maximum chromosome X LOD score of 0.30 is achieved at four regions. The red arrow indicates the location of *SPRTN*.

Nature Genetics: doi:10.1038/ng.3103

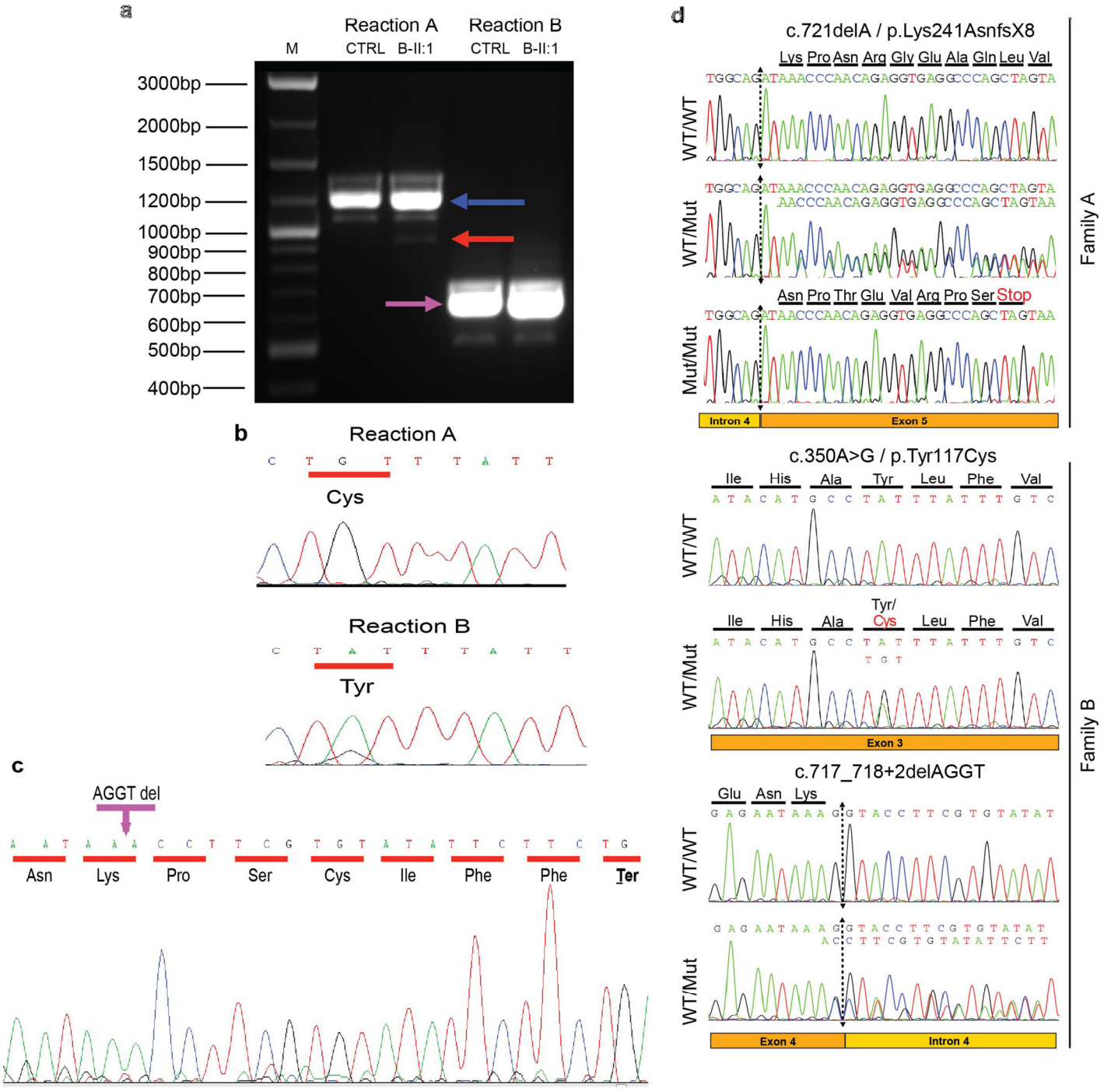

Supplementary Figure 2

RT-PCR analysis and Sanger sequencing.

(**a**) RT-PCR study of *SPRTN*. M indicates molecular marker. Reaction A, amplifying isoform 1, with primers in exon 2 and 5, revealed a full length allele of 1205bp (blue arrow) in both a healthy individual (CTRL) and B-

II:1. A very weak band (red arrow) corresponding to skipping of exon 4 (1205bp-268bp=937bp) is observed in B-II:1. Reaction B, amplifying isoform 2, with primers in exon 2 and intron 4 revealed a band at 640bp (pink arrow). (**b**) Sequence trace of the B-II:1. Reaction A amplified only the allele with the missense p.Tyr117Cys variant. Reaction B preferentially amplified the allele without the missense variant. (**c**) Sequencing of the reaction B in B-II:1 with reverse primer revealed the c.717_718+2delAGGT mutation, confirming that reaction B amplified only the allele including the 4bp deletion. Therefore the consequence of this deletion is mostly intron 4 inclusion causing p.Lys239LysfsX7. (**d**) Sequence chromatograms of all three identified mutations, after PCR amplification of genomic DNA. The amino acid translation is shown in the three-letter code above the chromatograms.

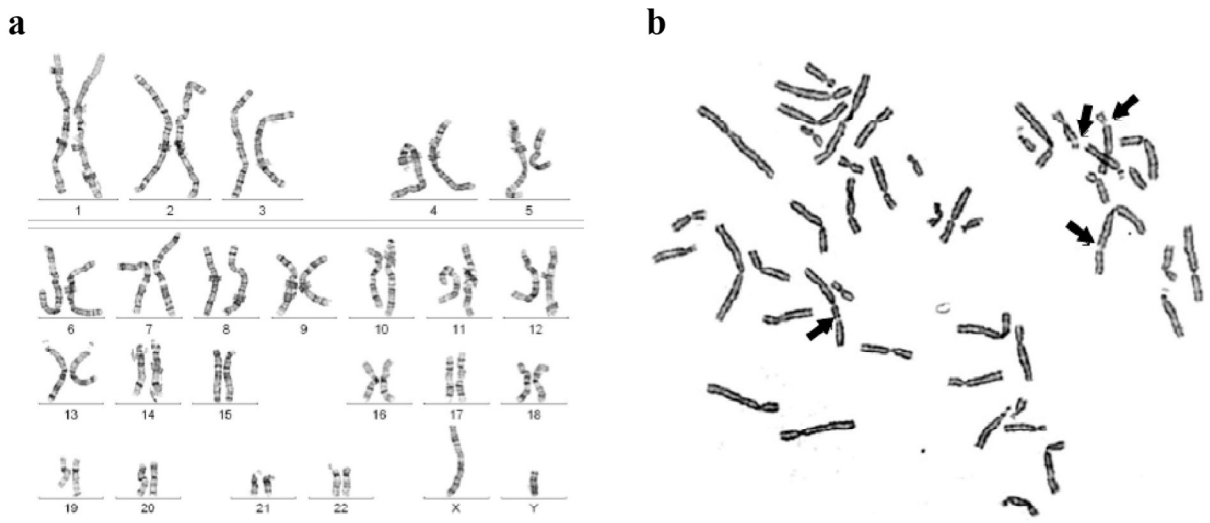

Supplementary Figure 3

Representative images of peripheral blood metaphase spreads of B-II:4.

(**a**) G-banded analysis of lymphocyte cells showed random, spontaneous breaks and unbalanced rearrangements, including deletions, acentric fragments and marker chromosomes in 13 of 30 cells analyzed. The remaining cells showed an apparently normal male karyotype. A representative abnormal karyotype shows 46,XY,del(5)(?q31.3). (**b**) Examination of solid stained metaphase chromosomes showed an abnormal level of spontaneous chromosome breakage (arrows). There were 39 breaks in 45 analyzed cells, while the control sample showed 3 breaks in 45 cells. A similar level of spontaneous breakage was observed in the other proband (B-II:1). G-banded analysis of lymphocyte cells showed random, spontaneous breaks and rearrangements, including translocations and deletions, in 14 of 25 cells analyzed (data not shown).

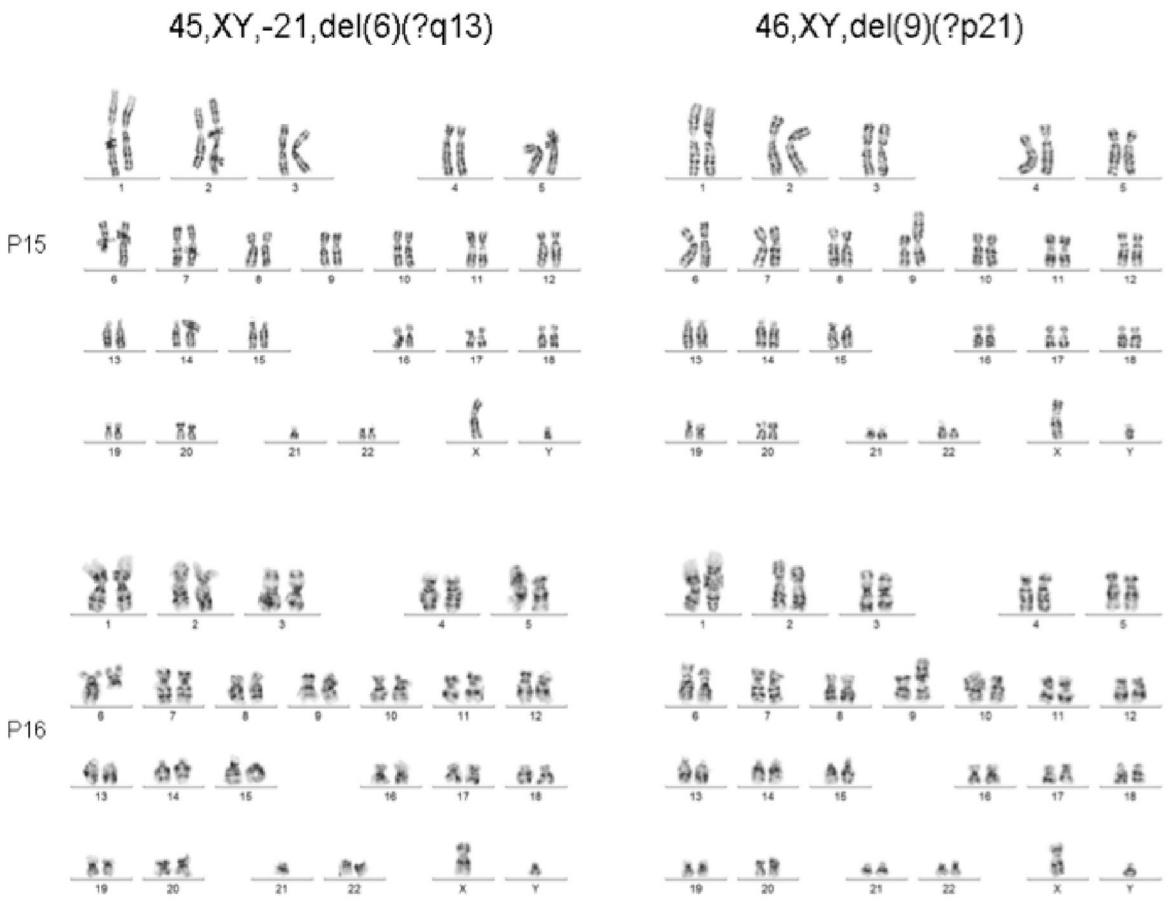

Supplementary Figure 4

Representative images of fibroblast metaphase spreads of B-II:1.

G-banded analysis of two subsequent B-II:1 fibroblast passages, 15 and 16, showed random, spontaneous breaks, balanced and unbalanced rearrangements, including deletions, acentric fragments and marker chromosomes in 9 of 30 cells analyzed from passage 15, and in 9 of 42 cells analyzed from passage 16. The remaining cells showed an apparently normal male karyotype. Depicted are two cytogenetically defined clones in both subsequent passages, 46,XY,del(9)(?p21) and 45,XY,-21,del(6)(?q13), the latter was identified in three metaphases of passage 16. Examination of solid stained metaphase chromosomes also showed an abnormal level of spontaneous chromosome breakage. There were 43 breaks in 47 analysed cells, while the control sample showed 1 break in 30 cells (data not shown).

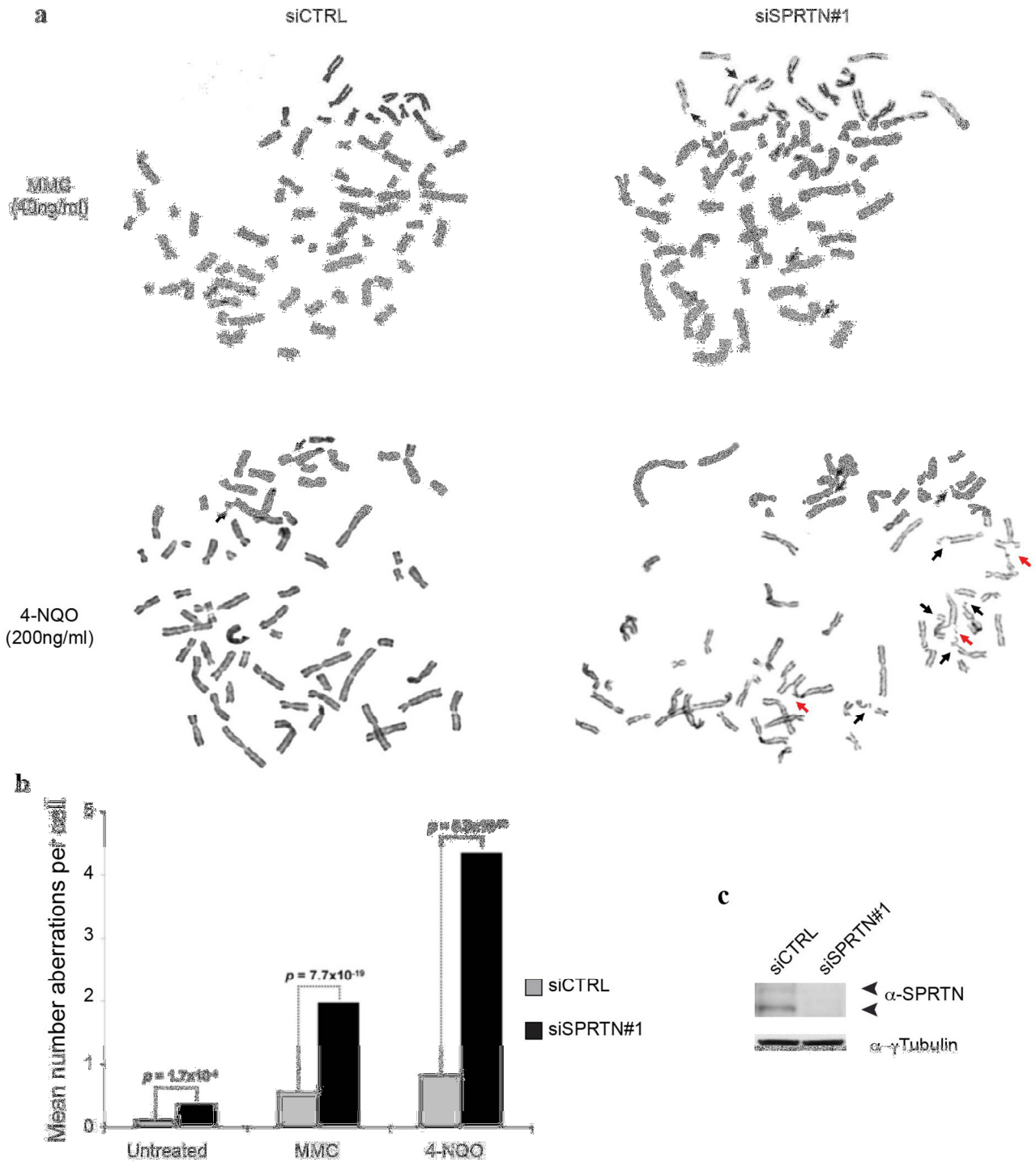

Supplementary Figure 5

Depletion of SPRTN by siRNA results in chromosomal instability.

(**a**) Representative images of metaphase spreads of siRNA transfected HEK293T cells. Black arrows indicate chromatid breaks. Red arrows indicate open multiradial figures each representing several chromatid breaks. (**b**)

Mean number of aberrations per cell observed in 100 metaphases of HEK293T cells transfected with siRNA alone or additionally treated either with 40ng/ml of MMC or 200ng/ml of 4-NQO. Bar graphs summarize three independent experiments. p-values are given above the graphs. (**c**) Depletion of SPRTN was confirmed by western blot. Tubulin was used as a loading control.

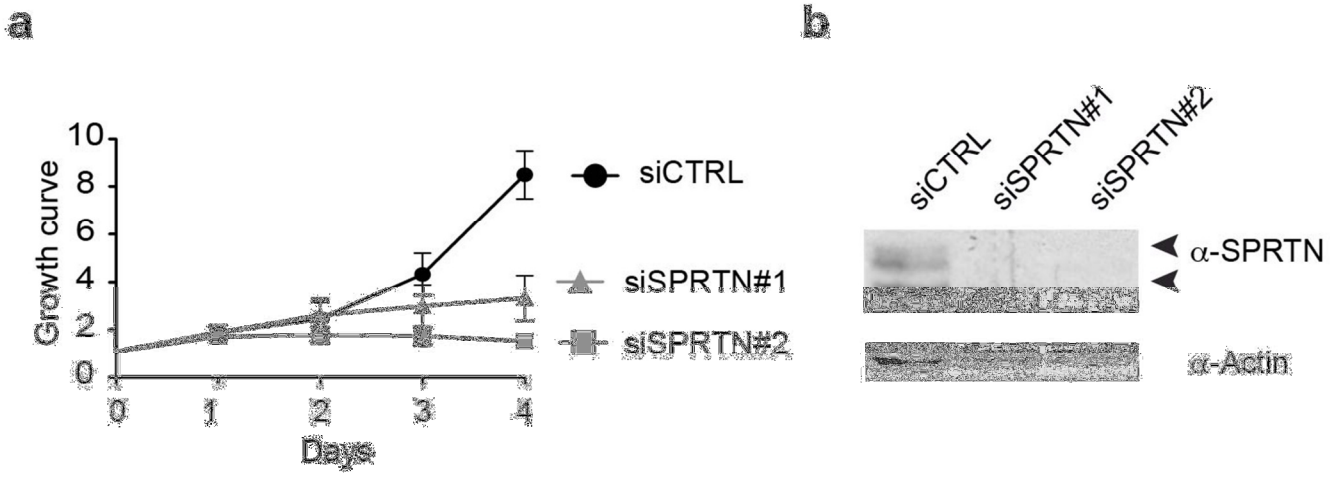

Supplementary Figure 6

SPRTN depletion suppresses cell proliferation.

(**a**) 50'000 of U2OS cells were seeded at day 0 and normalized to 1 (y-axis). Every 24 hours cells (x-axis) were washed, trypsinized, resuspended in 1mL medium and counted. The graph represents the mean +/- standard deviation of 3 independent experiments. Each experiment was performed in triplicate. (**b**) Efficacy of SPRTN depletion.

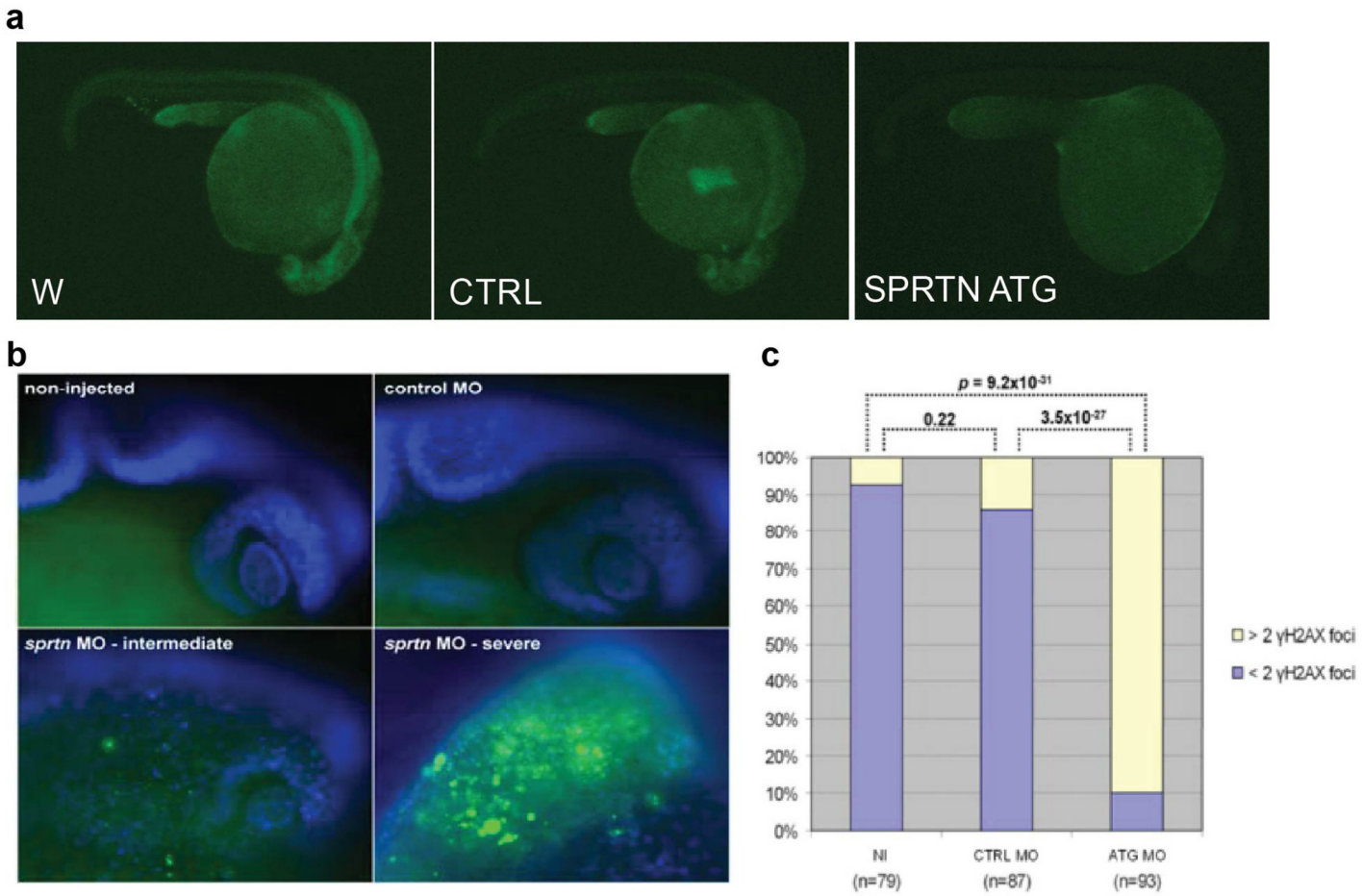

Supplementary Figure 7

SPRTN has an evolutionary conserved role in the DNA damage response.

(**a**) Morpholino specificity and efficacy demonstrated by knockdown of GFP reporter expression. Co-injection of the translation blocking antisense MO targeted against the 5'-UTR inhibited all GFP fluorescence, while coinjection of a 5 bases mismatch control MO did not repress fluorescence. (**b**) Lateral view of the head region of 27 hpf zebrafish embryos stained with zebrafish anti γ-H2AX (FITC). Nuclei were counterstained with DAPI (blue). Knockdown of sprtn with 1.5ng ATG MO significantly increases the staining for γ-H2AX, indicating increased DDR. (**c**) Quantification of γ-H2AX foci after sprtn downregulation in zebrafish. Bar graphs summarize three independent experiments. Statistical significance was determined using Fisher's exact test, p-values are given above the graphs. NI = non injection.

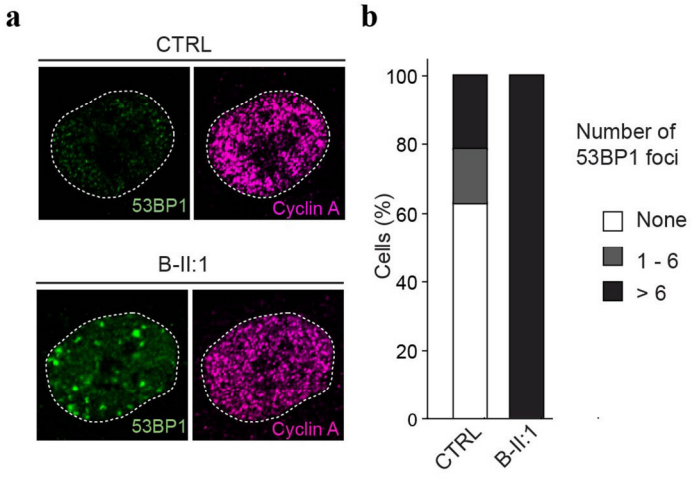

Supplementary Figure 8

Mutations in *SPRTN* cause elevated number of DNA double-strand breaks (DSBs) in S phase.

(**a**) Primary skin fibroblasts stained with the S-phase cell cycle marker (Cyclin A) and antibodies against 53BP1 (DNA double strand breaks marker). (**b**) The number of 53BP1 foci per cell in cyclin A positive cells was quantified in three independent experiments with greater than 100 cells scored per condition per experiment.

Nature Genetics: doi:10.1038/ng.3103

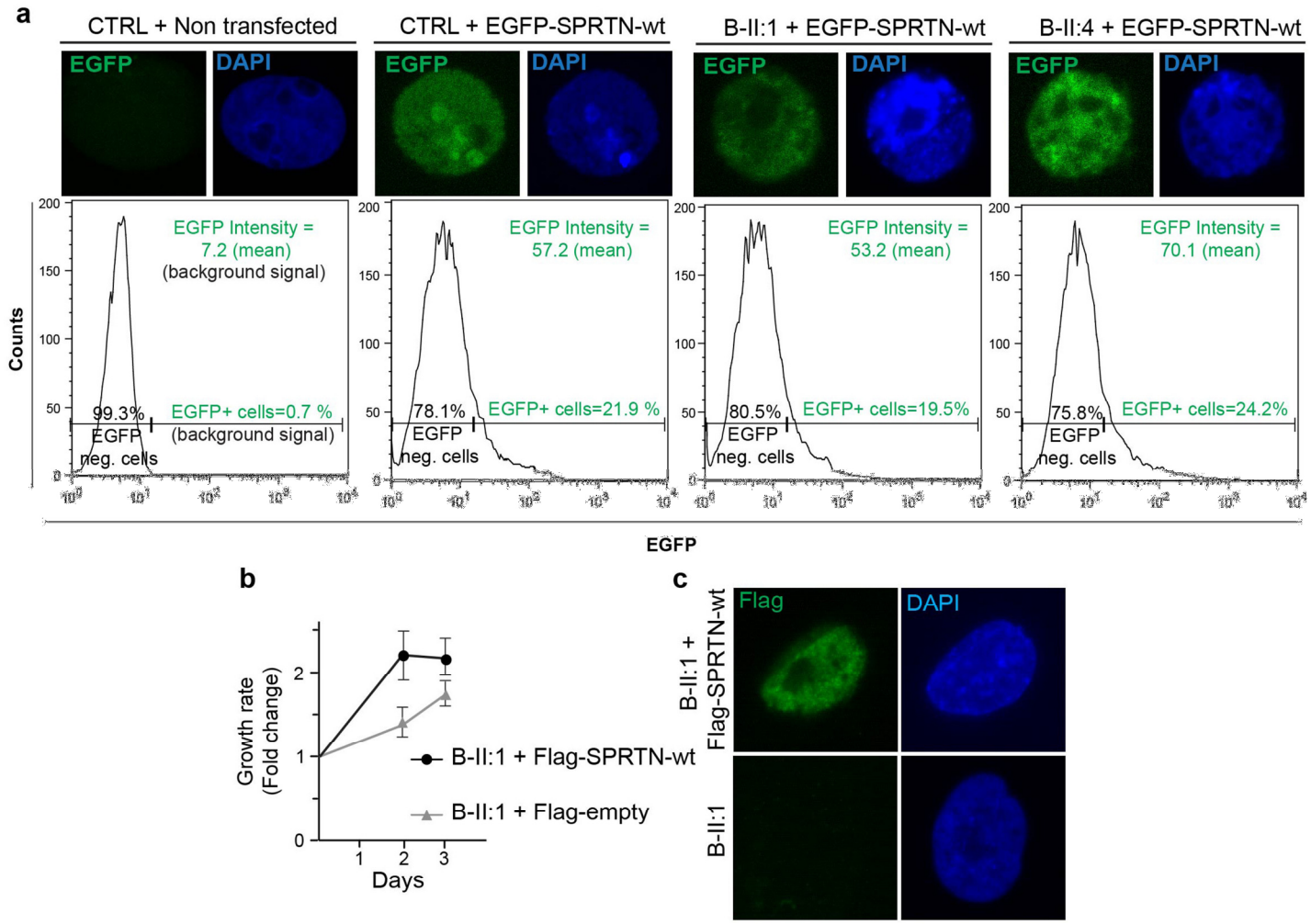

Supplementary Figure 9

Overexpression of WT SPRTN rescues DNA replication and proliferation phenotypes in patient LCLs and fibroblasts.

(**a**) The overexpression of EGFP-SPRTN-wt in stable transfected LCLs was confirmed by fluorescence microscopy (upper panel) and flow cytometry (lower panel). Note that only 20-24% of stable-transfected LCLs express EGFP-SPRTN. (**b**) Flag-SPRTN-wt or Flag-empty vector transiently transfected B-II:1 skin fibroblasts were seeded and growth curve was measured as indicated in Supplementary Fig. 6; three independent experiments, error bars; s.e.m. (**c**) Flag-SPRTN-wt expression in primary skin fibroblasts was confirmed by immunofluorescence analysis.

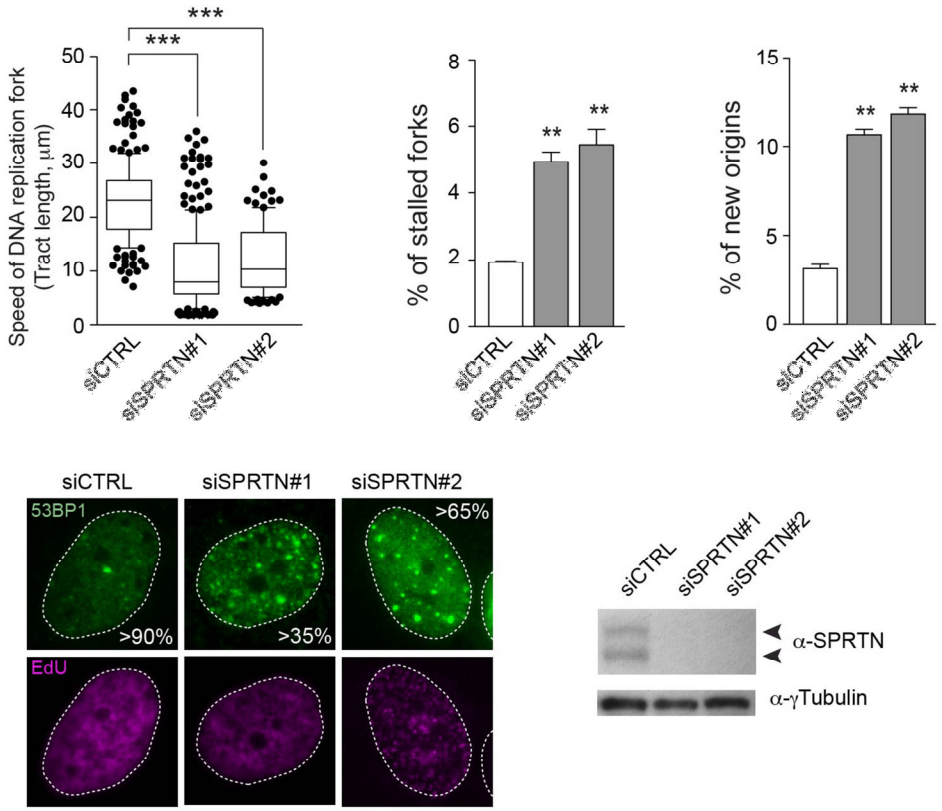

Supplementary Figure 10

Depletion of SPRTN causes DNA replication stress.

a) U2OS cells were treated with two independent siRNAs against SPRTN (siRNA-SPRTN#1 or siRNA-SPRTN#2) or control siRNA (siCTRL) and DNA replication forks were analyzed. The quantification from three independent experiments using the same methodology as in Figure 4 Panels a-d. (**b**) Representative cells with huge increase in the number of 53BP1 (markers of DSBs) foci in S-phase (EdU-positive; cells were grown in the presence of EdU for 30 min before fixation) of SPRTN-depleted U2OS cells. % of cells with depicted phenotypes when more than 100 cells were scored per condition in three independent experiments. (**c**) Efficacy of SPRTN depletion.

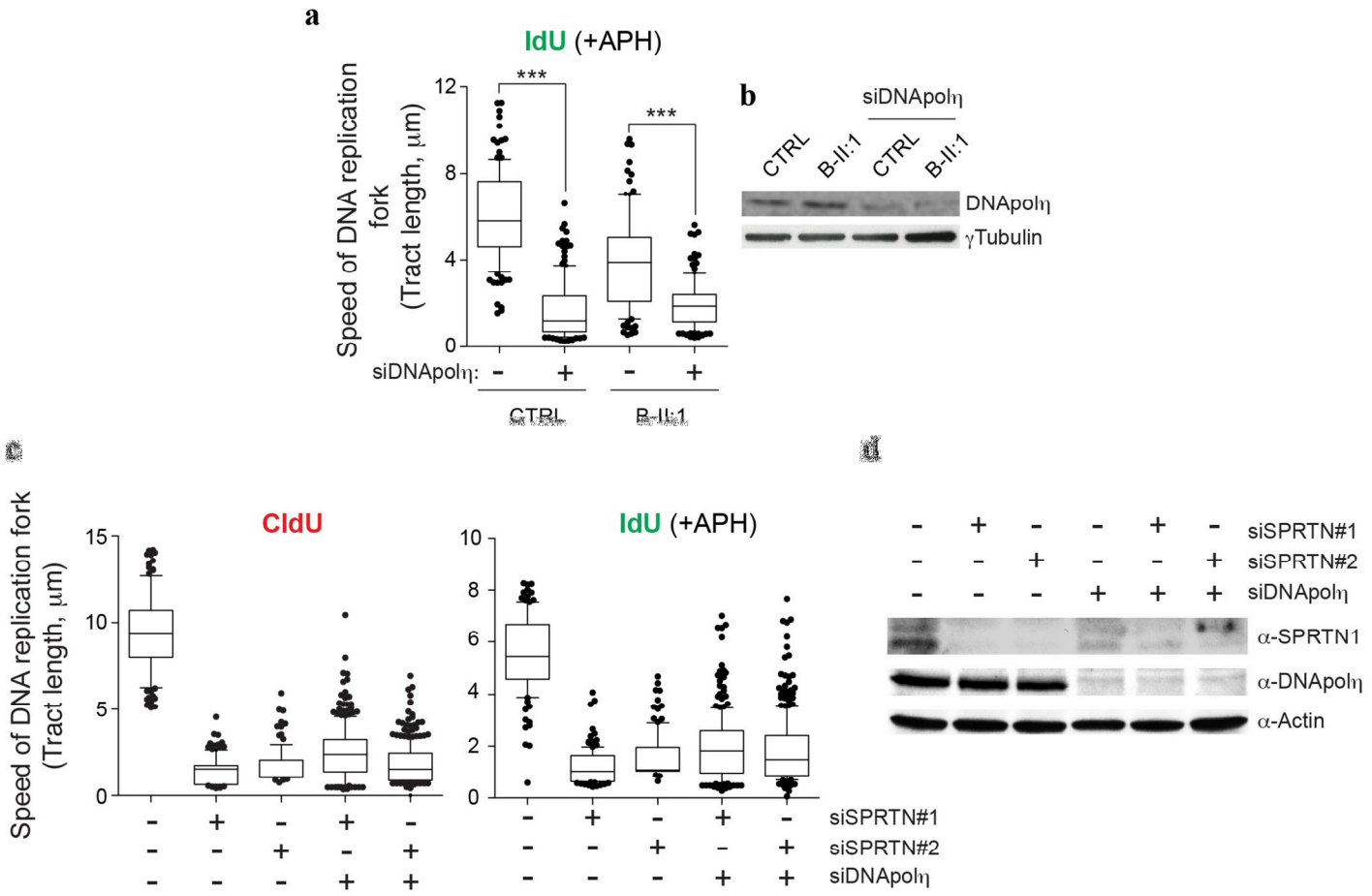

Supplementary Figure 11

Depletion of DNA polymerase η is unable to rescue the DNA replication defect in patient LCLs or SPRTN-depleted U2OS cells.

Analysis of DNA replication fork progression in patient cells or SPRTN-depleted U2OS cells +/- co-depletion of DNA polymerase η by DNA fiber assay as described earlier in the text. (**a**) DNA fiber analysis of patient LCLs in the presence of APH. (**b**) Efficacy of siRNA depletion as indicated. (**c**) DNA fiber analysis with (right panel) or without APH (left) in siRNA-depleted U2OS cells. Two independent experiments with 100 fibers per condition per experiment. (**d**) The efficacy of depletion

.

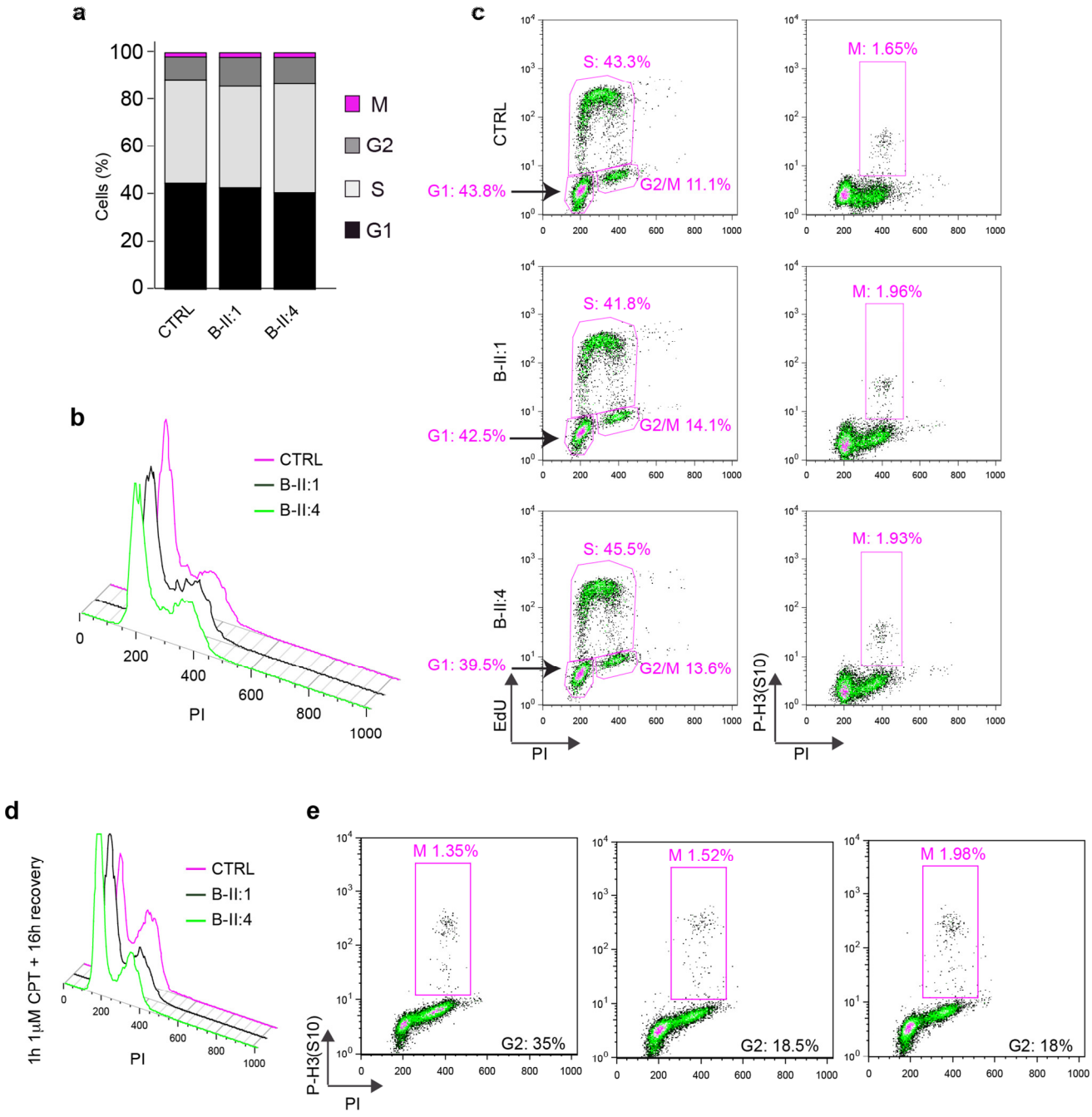

Supplementary Figure 12

Cell cycle profile of unchallenged or CPT-challenged patients' LCL cells.

(**a**) Graphic representation of the cell cycle distribution in control and patient LCLs. G_1, S, G_2 and mitotic (M) cells were determinated by flow cytometry based on the triple staining with propidium iodide (PI: DNA content), EdU (S-phase) and phosph-Ser10 histone H3 (marker for mitotic cells).(**b**) Representative histograms

for DNA content (PI). The *y*-axis represents cell counts and the *x*-axis represents DNA area. The first peak indicates cells in G_1 and the second peak indicates cells in G_2-M. Cells between two indicated peaks represent S-phase. (**c**) Representative dotplot distribution of EdU (left graph) or phospho-Ser10 histone H3 (right graph) positive cells (*y* axis) versus DNA content (*x* axis). (**d**) Graphic representation of the cell cycle distribution following induction of replication-related DSB (1μM CPT treatment for 1 hour and recovery for 16 hours). (**e**) Representative dotplot distribution of mitotic cells detected by p-H3(S10) and depicted in pink rectangles (% of M cells).

.

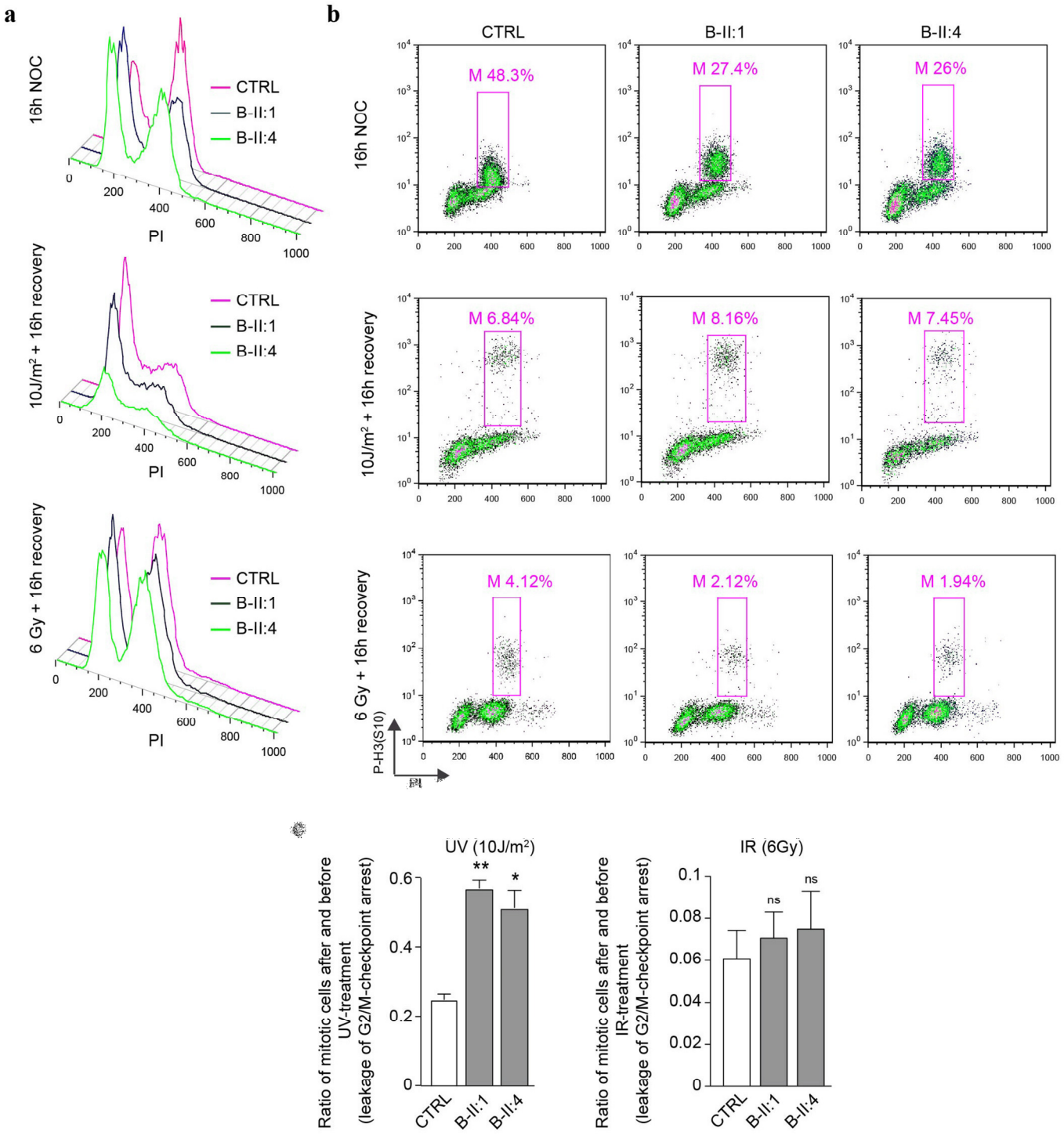

Supplementary Figure 13

G2/M checkpoint leakage following replication-related DSB but not ionizing radiation (IR)-induced DSB of patient LCLs.

(**a**) Cell cycle profile of patient cells before DNA damage or after UV-irradiation (10J/m^2) or IR (6 Gy)

treatment. The cells were allowed to recover for 16 hours in the presence of nocodazole and analysed by PI profile. (**b**) Representative dotplot distribution of phospho-Serine-10 histone H3 positive cells. (**c**) Due to proliferation defects observed in patient LCL's, G2-M checkpoint efficiency was expressed as the mitotic ratio between the number of mitotic cells after and before DNA damage. Note that G2/M-checkpoint is not properly functional in UV-treated patient LCLs (about 3-fold less mitotic cells after UV) when compared to control cells (7-fold less mitotic cells after UV). In contrary to UV, IR treatment (b and c) is equally efficient in both patient and control LCLs (about 12 fold).

Nature Genetics: doi:10.1038/ng.3103

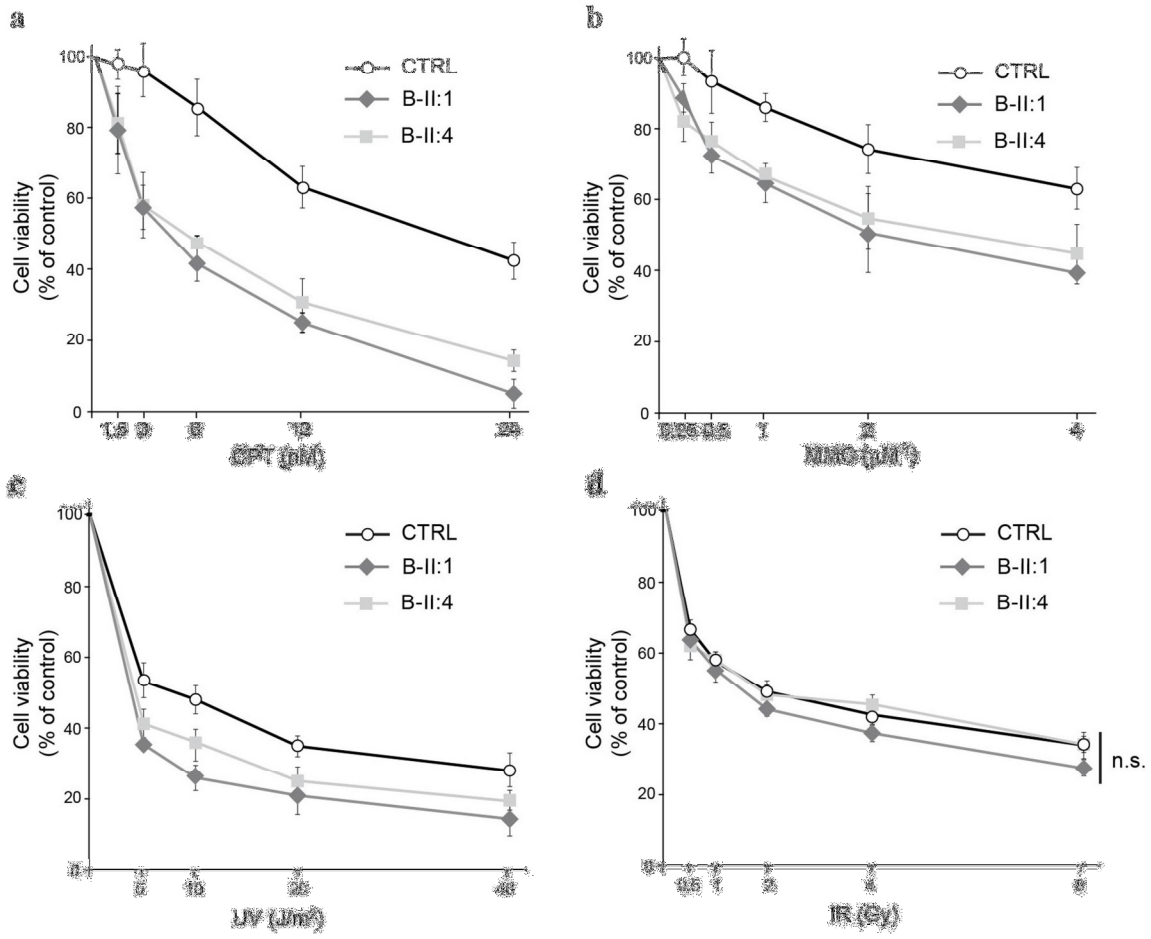

Supplementary Figure 14

Patient cells are hypersensitive to replication-related DNA damaging agents but not to IR.

Cell viability of control and patient LCL's after treatment with different DNA damaging agents: (**a**) Camptothecin (CPT), (**b**) Mitomycin C (MMC), (**c**) UV-radiation, and (**d**) ionizing radiation (IR), using a commercial MTT assay. The cells were treated for 48 hours with the indicated genotoxic agents and allowed to recover for 48 hours. (a-d) Three independent experiments, and each experiment was performed in triplicate. n.s. = not significant, unpaired t-test

.

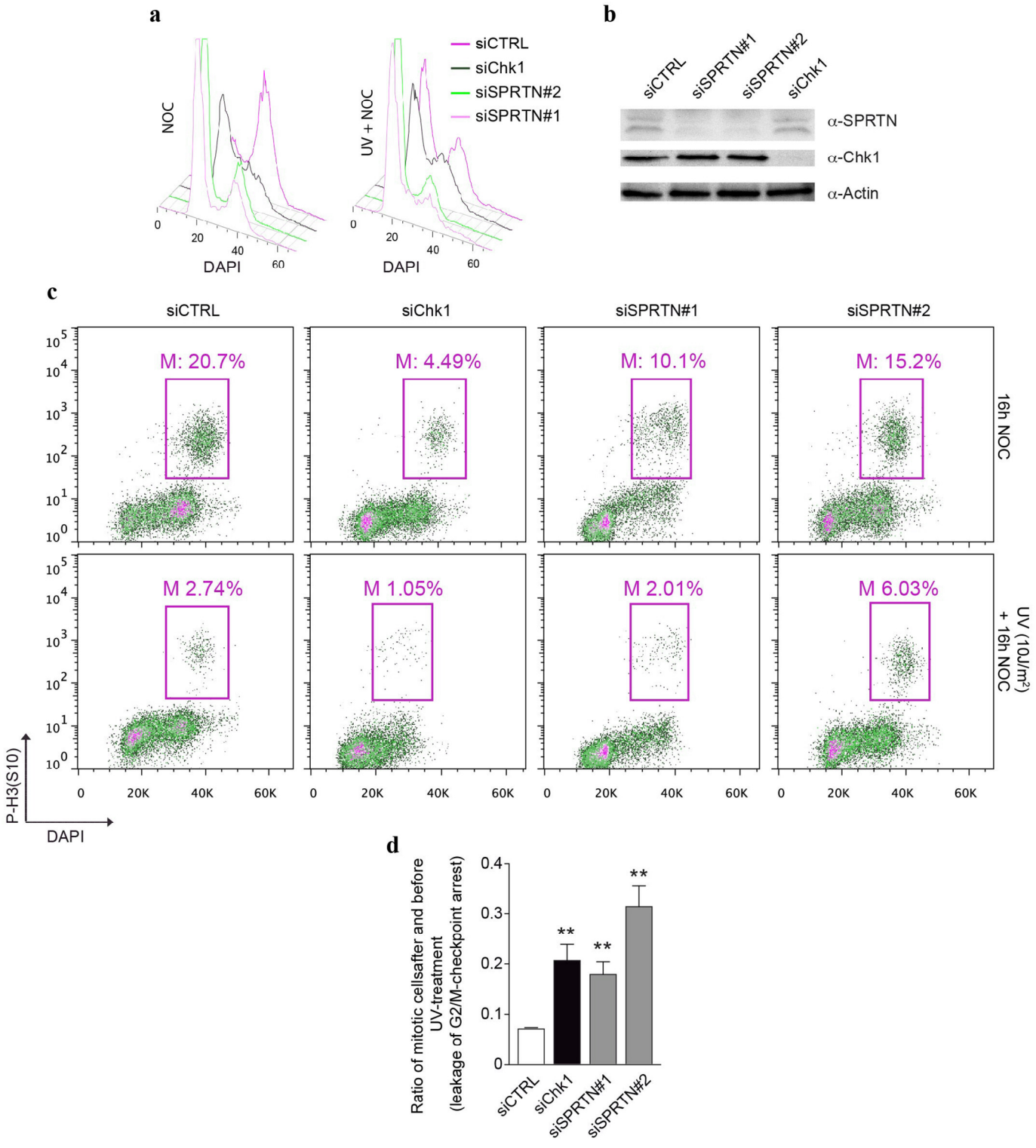

Supplementary Figure 15

Depletion of SPRTN causes G2/M-checkpoint leakage after UV in U2OS cells.

(**a**) Cell cycle profile analysed by DNA content (DAPI) of siRNA-depleted cells without or with UV-irradiation

in the presence of nocodazole (NOC). (**b**) Western blot analysis of siRNA-depletion efficacy. (**c**) A representative dotplot distribution of mitotic cells detected by p-H3(S10) and depicted in red rectangles (% of M cells). In control cells (siCTRL) there is approximately 8-fold less mitotic cells after UV comparing to unchallenged conditions (efficient G2/M-arrest), whereas in SPRTN-depleted cells there is only about 3-fold (SPRTN# 2) or 5-fold less (SPRTN#1). (**d**) To better visualize the G2/M-defect after UV-damage in DVC1-depleted cells mitotic cells were calculated and presented as a mitotic ratio after and before UV-treatment. Depletion of Chk1 was used as a positive control for G2/M leakage.

.

Nature Genetics: doi:10.1038/ng.3103

Supplementary Table 1a. Exome variant filtering in A-IV:1

Filter	Count
Total count of variations	425,316
Reaching minimal quality (>6 reads; Qual> 15)	118,166
Splice +/10bp or protein change, not in In-house DB, 1000genomes, MAF<0.01	525
Homozygous (Allele frequency >75%), MAF<0.01	73
Co-segregating in the family, MAF<0.01	11
Not in dbSNPv137	1
Protein truncating or splice site variant	1

Supplementary Table 1b. Exome variant filtering in B-II:4 under homozygous, hemizygous and compound heterozygous genetic models. AAF = alternate allele frequency.

Filter	No. variants
Total variants detected with quality ≥ 10	380,449
Variant quality≥ 13	283,748
Located within one of 33 linkage intervals	33,176
Rare (AAF ≤1% in the 1000 Genomes and NHLBI ESP6500 data sets, and AAF ≤4% in the Complete Genomics 69 data set and 132 in-house exomes)	5,531
Within 2 bp of splice site, or predicted to affect protein sequence	210
Pairs of compound or phase unknown heterozygous variants (Table S2B)	65*
Homozygous variants (Table S2C)	7
Hemizygous variants (Table S2D)	3

* Located in nine genes, one of which was *SPRTN*.

Nature Genetics: doi:10.1038/ng.3103

Supplementary Table 2a. Homozygous variants with minor allele frequencies (MAF) < 0.01 showing co-segregation in the family A.

Gene	Chromosome	Quality	Total Depth	Allele Freq.	Protein Change	dbSNP v137
MRPL55	1	39	18	89	Arg25His	rs74140967
MRPL55	1	51	8	100	Gly39Ser	rs76046017
GUK1	1	40	15	93	Arg118Trp	rs56280722
OBSCN	1	199	57	100	Arg467Cys	rs74142685
OBSCN	1	255	184	100	Thr1513Met	rs74142695
OBSCN	1	51	8	100	Gly2813Arg	rs74142687
OBSCN	1	81	18	100	Arg5693Met	rs80298121
OBSCN	1	51	8	100	Tyr7735Phe	rs77969788
SPRTN	**1**	**496**	**166**	**98**	**Lys241AsnfsX8**	**no**
RGPD1	2	51	8	100	Pro20Leu	rs201509849
CFTR	7	192	68	97	Leu997Phe	rs1800111

Nature Genetics: doi:10.1038/ng.3103

Supplementary Table 2b. Candidate compound heterozygous variants in family B. See Supplementary Table 1b for criteria used to identify candidates.

Gene	Chr.	Quality	Total Depth	Alternate Depth	Protein Change	dbSNP v137
E2F2	1	30	8	2	Asp430Gly	**no**
E2F2	1	266	18	11	Gly205Arg	rs2229297
EPHA8	1	200	23	8	Gly45Ser	rs45498698
EPHA8	1	412	28	20	Pro607His	rs144329757
PRAMEF2	1	622	297	56	Leu105Ter	rs78738981
PRAMEF2	1	579	131	47	Leu310Val	**no**
SPRTN	**1**	**836**	**77**	**36**	**Tyr117Cys**	**no**
SPRTN	**1**	**1844**	**52**	**26**	**Frameshift (c.717_718+2delAGGT)**	**no**
DOCK5	8	65	37	10	Splicing (c.976+2T>G)	rs77327996
DOCK5	8	64	14	4	Cys956Phe	rs201180829

Nature Genetics: doi:10.1038/ng.3103

Supplementary Table 2c. Candidate homozygous variants in family B. See Supplementary Table 1b for criteria used to identify candidates.

Gene	Chr.	Quality	Total Depth	Alternate Depth	Protein Change	dbSNP v137
SLC45A1	1	15	1	1	Ala705Gly	no
AOAH	7	18	12	8	Leu640Profs*26	no
UBXN8	8	1802	67	64	Arg207Ser	rs77443237
AMER2	13	19	2	2	Lys168Asn	no
CES1	16	158	18	12	Splicing (c.1087-2dupT)	no
EXOC3L1	16	116	4	4	Tyr75Asn	rs117403380
PKD1L3	16	2998	50	47	Lys1233Asnfs*21	rs149635567

Supplementary Table 2d. Candidate hemizygous variants in family B. See Supplementary Table 1b for criteria used to identify candidates.

Gene	Chr.	Quality	Total Depth	Alternate Depth	Protein Change	dbSNP v137
MXRA5	X	378	12	12	Arg2734Gln	rs144024869
WDR13	X	19	2	2	Gln53Lys	no
MAGEC3	X	704	21	21	Val567Phe	rs143730187

Nature Genetics: doi:10.1038/ng.3103

Supplementary Table 3. Co-segregation at the *SPRTN* locus

Family A	
A-III:1	c.721delA / wt
A-III:2	c.721delA / wt
A-IV:1	c.721delA / c.721delA
A-IV:2	c.721delA / wt
Family B	
B-I:1	c.717_718+2delAGGT / wt
B-I:2	c.350A>G / wt
B-II:1	c.717_718+2delAGGT / c.350A>G
B-II:2	c.717_718+2delAGGT / wt
B-II:3	c.717_718+2delAGGT / wt
B-II:4	c.717_718+2delAGGT / c.350A>G

Nature Genetics: doi:10.1038/ng.3103

Supplementary Table 4. DNA primers used in this study.

SPRTN **primer for reverse transcription PCR:**
SPRTN-2F 5'-CCATCCGTCTCAGCGAACC-3'
SPRTN-5R 5'-CAAAAGCGAAGAAAGTCTTGA-3'
SPRTN-4R 5'-gagcaaagtctgttttcctaccatc-3'
Primer for amplification of zebrafish ***SPRTN:***
Forward 5'- CGTTGACATCTTTAGCTCCACACT-3`
Reverse 5'-CGTCTTGAGACCATTTCCGCCTAT-3`
Zebrafish ***SPRTN*** **3'RACE PCR primer:**
Forward 5'-CCACAGACAAGAAACGAGAGGAGGTCAGAA-3'
Reverse 5'-AGCAGGCAAACAATCCTCCAGCCCAAATCA-3'
Primers used for cloning of human ***SPRTN*** **from pFLAG-CMV into pCRII-TOPO:**
forward 5'-GGATCCATGGATGATGACTTGATGTTG-3'
reverse 5'-CTCGAGTCAAAGACTTTCTTCGCTTTTG-3'
Zebrafish mutagenesis primer:
c.721Adel forward 5'-CAGAGAATAAAGATAACCCAACAGAGGTGAGGC-3'
c.721Adel reverse 5'-GCCTCACCTCTGTTGGGTTATCTTTATTCTCTG-3'
c.350A>G forward 5'-CTGCATGAAATGATACATGCCTGTTTATTTGTCACTAATAACGAC-3'
c.350A>G reverse 5'-GTCGTTATTAGTGACAAATAAACAGGCATGTATCATTTCATGCAG-3'

Nature Genetics: doi:10.1038/ng.3103

Supplementary Table 5. Antisense morpholino oligonucleotides and siRNA.

Zebrafish *SPRTN* RNA antisense morpholino oligonucleotides (MO)
ATG MO 5'- GAAGATGATGGAGGATGAAGACTTT-3'
splice-site MO 5'- CACATCTGAGGAAGAGAAACATTGA-3'
CTRL MO 5'- GAACATCATGGACGATCAAGAGTTT -3'
siRNA sequences
siSPRTN#1 : 5`-UCAAGGAACCAGAGAAUUATT-3` (Microsynth)
siSPRTN#2: 5'-AAUACAGGUGGUACUUGAGACUUUG-3' (Microsynth)[1]
siCHK1: 5'-AAGCGUGCCGUAGACUGUCCATT-3' (Microsynth)
siPOLH: 5'CUGGUUGUGAGCAUUCGUGUATT-3' (Microsynth)[46]
siNS was obtained fromQiagen

Nature Genetics: doi:10.1038/ng.3103